Synthesis and characterisation of bis(amino)silylene–nickel(0), –palladium(II), –platinum(0), –platinum(II) and copper(I) complexes

Anthony G. Avent, Barbara Gehrhus, Peter B. Hitchcock, Michael F. Lappert *, Hieronim Maciejewski [1]

The Chemistry Laboratory, University of Sussex, Brighton, BN1 9QJ, UK

Abstract

The bis(amino)silylene $Si[(NCH_2^tBu)_2C_6H_4-1,2]$ ($\equiv$ SiNN) behaved as a ligand in displacing COD or PPh_3 from $[Ni(COD)_2]$, $[Pt(PPh_3)_4]$ or $[CuI(PPh_3)_3]$, yielding the crystalline d^{10} complexes $[Ni(SiNN)_4]$ (crystallised from Et_2O as the 1:1-adduct **2**), $[Pt(PPh_3)(SiNN)_3]$ (**5**) or $[CuI(PPh_3)_2(SiNN)]$ (**6**). Under the same conditions (in C_6H_6 at ambient temperature), SiNN and $[MCl_2(PPh_3)_2]$ yielded the crystalline (i) d^8 complex *trans*-$[M\{SiNN(Cl)\}_2(SiNN)_2]$ [M = Pt (**3**), Pd (**4**)] or (ii) the d^{10} complexes $[Ni(PPh_3)_{4-n}(SiNN)_n]$ ($n = 4$ (**2**) or 3 (**1**), depending on stoichiometry; with Cl_2SiNN as co-product). The X-ray structures of **2**, **4**, **5** and **6** are presented; those of **1** and **3** appeared in a preliminary communication. Compound **3** was shown to undergo three fluxional processes in $CDCl_3$ solution, as shown by detailed variable temperature NMR spectroscopic experiments. These involved in order of increasing energy (a) two conformers of **3**, (b) one of these and the *cis*-isomer, and (c) $Si \rightarrow Si$ 1,3-shifts of Cl^-. These results are placed into the context of related published silylenemetal chemistry.
© 2003 Elsevier B.V. All rights reserved.

Keywords: Nickel; Palladium; Platinum; Copper; Silylene complexes; Silyl complexes

1. Introduction

There are several early reviews dealing with silylene-transition metal complexes $L_nM-SiXX'$ (X and X' being a monodentate anionic ligand); these were generally required to be stabilised by the incorporation of a neutral donor ligand D, as in $L_nM-Si(XX')D$ [1–3]. The first base-free silylenemetal complex [RuCp*(P-Me_3)\{Si(SR)_2\}][BPh_4] (Cp* = η^5-C_5Me_5, R = Et, C_6H_4Me-4) was reported by Tilley and co-workers in 1990 [4]. Further examples of cationic silylene complexes of Ru(II) and Pt(II) followed [5]. Each was obtained from a silylmetal precursor $L_nM-SiX_2(X')$ by abstraction of X'^-. Their stability was attributed mainly to π-donation from the heteroatom (e.g. S) bound to silicon [6]. The first, and thus far we believe the sole, instance of

the trapping of a transient silylene SiX_2 at a transition metal led to the complex $[Pt(PR_3)_2(SiMes_2)]$ (R = ^iPr, c-C_6H_{11}; Mes = $C_6H_2Me_3$-2,4,6), obtained by irradiating a mixture of $[Pt(PR_3)_3]$ and $SiMes_2(SiMe_3)_2$ [7].

A new chapter in SiX_2 chemistry was inaugurated in 1994 with the discovery by Denk, West, Haaland and their collaborators of the synthesis and gas phase structure of the first robust silylene $Si[N(^tBu)CH]_2$ (abbreviated as SiN^1N^1) [8], which was followed shortly thereafter by the synthesis and X-ray structure of the crystalline $Si[(NCH_2^tBu)_2C_6H_4-1,2]$ (SiNN) [9]. These two bis(amino)silylenes SiN^1N^1 and SiNN, as well as $Si[N(^tBu)CH_2]_2$ (SiN^2N^2), have been shown to have an extensive chemistry, as summarised in recent reviews [10,11]. Like bis(amino)-carbenes [12,13], -germylenes [14], -stannylenes [14] and -plumbylenes [14], each is capable of behaving as a ligand. This was first demonstrated in 1994 by the isolation (from $[Ni(CO)_4]$ and SiN^1N^1) and X-ray structure of $[Ni(CO)_2(SiN^1N^1)_2]$ [15] and later of $[Fe(CO)_4(SiN^1N^1)]$ [16]. We showed in 1997 that the silylene SiNN was capable of displacing a tertiary phosphine or an alkene from $[NiCl_2(PPh_3)_2]$ or

[Ni(COD)$_2$], respectively, in generating the crystalline silylene complexes [Ni(PPh$_3$)(SiNN)$_3$] and [Ni(SiNN)$_4$] [17]. Now almost thirty such compounds are known, as summarised in Section 3.

As had earlier been demonstrated for stannylenes such as Sn[N(SiMe$_3$)$_2$]$_2$ [14], the role of a bis(amino)metallene in transition metal chemistry is not limited to that of functioning as a ligand: it may insert into a transition metal M–X (e.g. X = Cl) bond, or alternatively act as a reducing agent. For the bis(amino)silylene SiNN the insertion reaction was illustrated by the conversion of [PtCl$_2$(PPh$_3$)$_2$] with SiNN into trans-[Pt{SiNN(Cl)}$_2$(SiNN)$_2$]; while the reduction was established by the dechlorination of [NiCl$_2$(PPh$_3$)$_2$] by SiNN to give [Ni(PPh$_3$)(SiNN)$_3$] and SiCl$_2$[(NCH$_2^t$Bu)$_2$C$_6$H$_4$-1,2] [17]. The three types of SiX$_2$ behaviour are illustrated schematically in Scheme 1. The insertion and reduction reactions of SiX$_2$ have not yet been widely explored; two complexes of the former are cited in Section 3.

2. Results and discussion

In a preliminary publication we showed that the bis(amino)silylene SiNN (four equivalents) with one equivalent each of [NiCl$_2$(PPh$_3$)$_2$], [Ni(COD)$_2$], or [PtCl$_2$(PPh$_3$)$_2$] afforded the crystalline complexes [Ni(PPh$_3$)(SiNN)$_3$] (1), [Ni(SiNN)$_4$] (2), or trans-[Pt{SiNN(Cl)}$_2$(SiNN)$_2$] (3), while from SiNN (five equivalents) and [NiCl$_2$(PPh$_3$)$_2$] the product was 2; the X-ray structures of 1 and 3 were presented [17]. In this paper we provide (i) full details of these syntheses and extensions to those of trans-[Pd{SiNN(Cl)}$_2$(SiNN)$_2$] (4), [Pt(PPh$_3$)(SiNN)$_3$] (5) and [CuI(PPh$_3$)$_2$(SiNN)] (6), (ii) X-ray structural information on 2, 4, 5 and 6, and (iii) detailed multinuclear NMR spectral data on each of 1–6 (which leads us to revise our original view as to the structure of 3 in CDCl$_3$); some of these results were
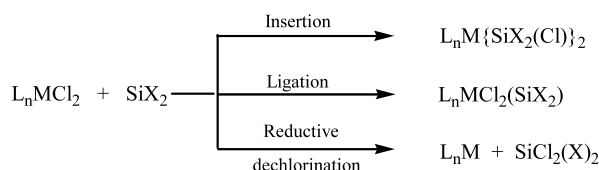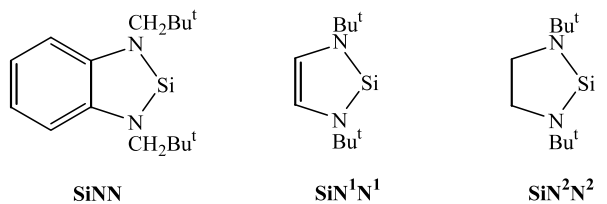
briefly alluded to in our review [11]. Previously we also reported that SiNN formed crystalline 1:1-adducts with [LnCp$_3$] (Ln = Y or Yb), which in toluene-d_8 readily dissociated (Y > Yb) [18].

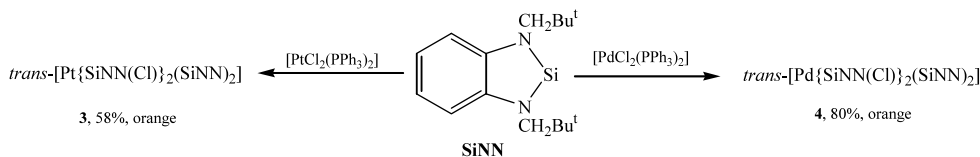### 2.1. Ligation reactions of the bis(amino)silylene SiNN

The reactions of SiNN with the appropriate Ni(0), Pt(0) or Cu(I) complex in the molar ratio 4:1, 3:1 or 1.5:1, respectively, gave in good yield the crystalline bis(amino)silylenemetal complex 2, 5 and 6, respectively, as summarised in Scheme 2. Each experiment was carried out in benzene at ambient temperature, demonstrating that in these systems the silylene SiNN readily displaced cycloocta-1,5-diene or triphenylphosphine from the appropriate d^{10} metal centre.

2.2. Reactions of the bis(amino)silylene involving ligation and concomitant insertion

Using reaction conditions identical to those of Section 2.1, treatment of [MCl$_2$(PPh$_3$)$_2$] with four equivalents of SiNN gave the crystalline trans-bis(chlorosilyl)bis(silylene)metal(II) complex 3 (M = Pt) or 4 (M = Pd), as summarised in Scheme 3. It is evident that in the formation of these d^8 metal complexes, the bis(amino)silylene behaved not only as a ligand but also a coordinatively unsaturated moiety gaining coordinative saturation by inserting into the appropriate M–Cl bond. It is likely that the formation of the coordinated bis(amino)(chloro)silyl ligand proceeded via intermediates having M bound to mutually cisoid SiNN and Cl$^-$ ligands. Whether the triphenylphosphine is first displaced generating labile complexes MCl$_2$(PPh$_3$)$_{2-n}$-(SiNN)$_n$ (n = 1 or 2) remains an open question. These insertion/ligation reactions may be compared with the behaviour of [{PtCl(μ-Cl)(PEt$_3$)}$_2$], which with an excess of Sn[N(SiMe$_3$)$_2$]$_2$ or Sn[CH(SiMe$_3$)$_2$]$_2$ gave [{Pt{Sn-(N(SiMe$_3$)$_2$)$_2$Cl}(μ-Cl)(PEt$_3$)}$_2$], (cis- and trans-; trans-on heating) or trans-[PtCl{Sn(CH(SiMe$_3$)$_2$)$_2$Cl}-(PEt$_3$){Sn(CH(SiMe$_3$)$_2$)$_2$}] (trans-Sn/Sn′), respectively [19].

SiNN **SiN^{1}N^1** **SiN^{2}N^2**
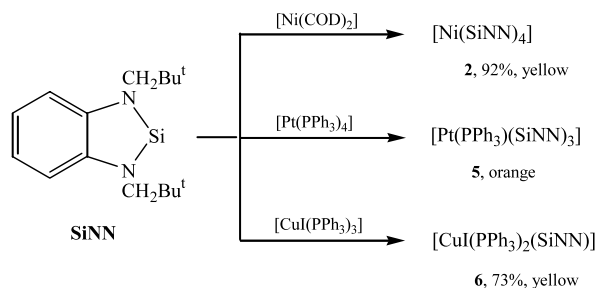
Scheme 1.

Scheme 2.

Scheme 3.

2.3. Reactions of the bis(amino)silylene involving ligation and concomitant reduction

Under reaction conditions identical to those of Sections 2.1 and 2.2, treatment of [NiCl$_2$(PPh$_3$)$_2$] with four or five equivalents of SiNN gave the crystalline bis(amino)silylenenickel(0) complexes **1** or **2**, respectively; likewise NiCl$_2$ was a ready source of **2**. These data are summarised in Scheme 4. By NMR experiments it was established that the reductive dechlorination of the d^8 Ni(II) substrate was accompanied by the concomitant oxidation of the silylene to yield the silane SiCl$_2$[(NCH$_2^t$Bu)$_2$C$_6$H$_4$-1,2] [20]. The contrast between the behaviour of [NiCl$_2$(PPh$_3$)$_2$] and its heavier d^8 congeners [MCl$_2$(PPh$_3$)$_2$] (M = Pd, Pt) (Scheme 3) is noteworthy. That a Pt(II) chloride was more resistant to reductive dechlorination than an isoleptic Pd compound was previously demonstrated: [MCl$_2$(COD)] with an excess of Sn[N(SiMe$_3$)$_2$]$_2$ gave [Pd{Sn(N(SiMe$_3$)$_2$)$_2$}$_3$] for M = Pd but cis-[Pt{Sn(N(SiMe$_3$)$_2$)$_2$Cl}$_2$(COD)] for M = Pt [21].

2.4. The X-ray structures of the crystalline compounds 2, 4, 5 and 6

The molecular structures of the compounds [Ni(PPh$_3$)(SiNN)$_3$] **1** and trans-[Pt{SiNN(Cl)}$_2$(SiNN)$_2$] **3** have been published [17]. In summary; compound **1** lies on a crystallographic threefold axis, with the Si–Ni–P angles of 106.4(1)° narrower than the Si–Ni–Si angles of 112.4(1)°, the Si–Ni and P–Ni distances of 2.165(2) and 2.210(4) Å, respectively, and each silicon atom is 0.214 Å out of the corresponding NiN$_2$ plane. The centrosymmetric compound **3** has Pt–SiNN and Pt–SiNN(Cl) bond lengths of 2.266(1) and 2.426(1) Å, respectively, the silicon atom of each SiNN ligand is only 0.04° out of the PtN$_2$ plane, and in each silylene ligand the neopentyl substituents are trans-disposed to one another (cf., cis- in **1**).

Crystalline **2** has the nickel atom at the centre of a distorted NiSi$_4$ tetrahedron, with three of the Si–Ni–Si′

bond angles close to the sp^3 value (110.7 ± 2.5°), two others much more acute (102.7 ± 1.8°), and Si(4)–Ni–Si(1) close to the sp^2 value at 119.77(6)°, Fig. 1. Selected geometrical parameters are in Table 1. Two of the Si–Ni bonds are significantly shorter than those to Si(1) or Si(4), and these may be compared (see Section 3) with those in **1** [17], [Ni(SiN^{1}N^1)$_3$] and [Ni(SiN^{2}N^2)$_3$] [22,23] and [Ni(CO)$_2$(SiN^{1}N^1)$_2$] [15,23]. The silicon atom of each SiNN ligand in **2** is 0.35–0.52 Å out of the appropriate NiN$_2$ plane, and each silylene ligand has the neopentyl ligands arranged cis to one another.

The labile compounds Pd(SiN^{1}N^1)$_3$ (δ[^{29}Si] = 113.6) and Pd(SiN^{2}N^2)$_3$ were believed to be intermediates along the pathway to [{Pd(P^{t}Bu$_3$)(μ-SiN^{1}N^1–Si or μ-SiN^{2}N^2–Si)}$_2$] from Pd(P^{t}Bu$_3$)$_2$ and SiN^{1}N^1 or SiN^{2}N^2 [24]; a related tetravalent silicon compound, [{Pd(PPh$_3$)-(μ-SiN^{1}N^1–Si)}$_2$], was made from [Pd(PPh$_3$)$_4$] and SiN^{1}N^1 [25]. However, the centrosymmetric crystalline d^8 complex **4** is the first crystallographically characterised palladium complex containing a silylene ligand free of neutral donor stabilisation, and is isomorphous
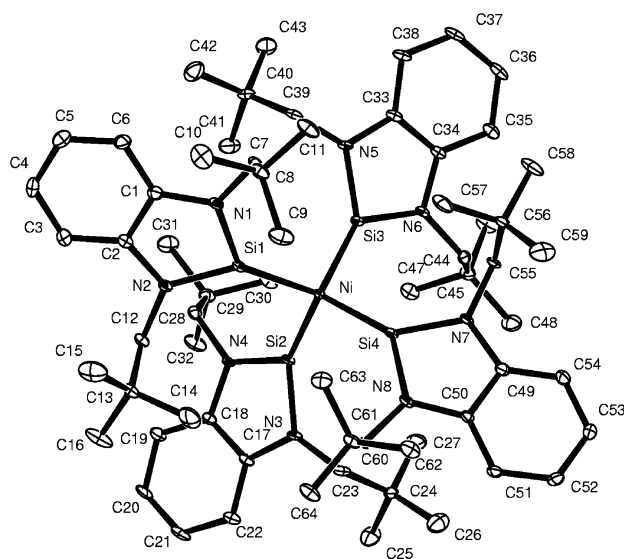
Fig. 1. Molecular structure of complex **2**.
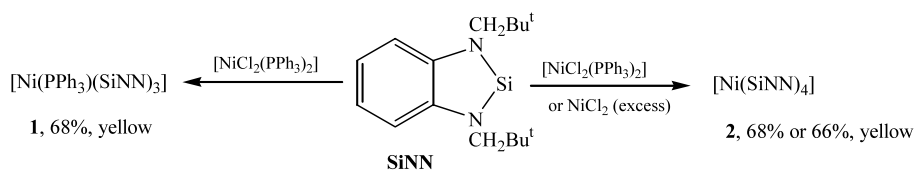
Scheme 4.

Table 1
Selected bond lengths (Å) and angles (°) for **2**

Bond lengths			
Ni–Si(1)	2.215(2)	Ni–Si(2)	2.110(2)
Ni–Si(3)	2.119(2)	Ni–Si(4)	2.196(2)
Si(1)–N(1)	1.754(4)	Si(1)–N(2)	1.757(4)
Si(2)–N(3)	1.714(4)	Si(2)–N(4)	1.760(4)
Si(3)–N(5)	1.722(4)	Si(3)–N(6)	1.777(4)
Si(4)–N(8)	1.734(4)	Si(4)–N(7)	1.762(4)
Bond angles			
Si(2)–Ni–Si(3)	113.16(6)	Si(2)–Ni–Si(4)	108.18(6)
Si(3)–Ni–Si(4)	103.67(6)	Si(2)–Ni–Si(1)	101.64(6)
Si(3)–Ni–Si(1)	110.74(6)	Si(4)–Ni–Si(1)	119.77(6)
N(1)–Si(1)–N(2)	86.0(2)	N(5)–Si(3)–N(6)	92.1(2)
N(3)–Si(2)–N(4)	91.5(2)	N(8)–Si(4)–N(7)	86.4(2)
N(1)–Si(1)–Ni	136.1(2)	N(3)–Si(2)–Ni	132.7(2)
N(2)–Si(1)–Ni	136.4(2)	N(4)–Si(2)–Ni	132.46(14)
N(5)–Si(3)–Ni	133.0(2)	N(7)–Si(4)–Ni	134.25(14)
N(6)–Si(3)–Ni	133.39(14)	N(8)–Si(4)–Ni	136.9(2)

Table 2
Selected bond lengths (Å) and angles (°) for **4**

Bond lengths			
Pd–Si(1)	2.269(2)	Pd–Si(2)	2.437(2)
Si(1)–N(1)	1.713(5)	Si(2)–N(3)	1.758(5)
Si(1)–N(2)	1.708(5)	Si(2)–N(4)	1.753(5)
Cl–Si(2)	2.105(2)		
Bond angles			
Si(1)–Pd–Si(1)′	180.0	Si(1)–Pd–Si(2)	90.79(7)
Si(2)–Pd–Si(2)′	180.0	Si(1)–Pd–Si(2)′	89.21(7)
N(2)–Si(1)–N(1)	92.6(2)	N(4)–Si(2)–N(3)	89.7(2)
N(1)–Si(1)–Pd	131.6(2)	N(4)–Si(2)–Cl	109.6(2)
N(2)–Si(1)–Pd	135.6(2)	N(3)–Si(2)–Cl	108.0(2)
N(3)–Si(2)–Pd	125.3(2)	Cl–Si(2)–Pd	99.94(8)
N(4)–Si(2)–Pd	123.7(2)		

Symmetry transformations used to generate equivalent atoms: $-x$, $-y$, $-z$.

with the isoleptic platinum(II) complex **3**, Fig. 2 and Table 2. The Pd–SiNN and Pd–SiNN(Cl) bond lengths of 2.269(2) and 2.437(2) Å, respectively, are closely similar to those in **3**; and the latter is in the upper range previously found (2.33–2.43 Å) for Pd–silyl distances [26,27]. As in **3**, the neopentyl substitutents in each silylene ligand are *trans* to one another, probably in order to accommodate the mutually *trans* chlorine atoms on the adjacent silyl ligands.

The crystalline d[10] platinum(0) complex **5** lies on a threefold symmetry axis; it is isomorphous with the isoleptic Ni(0) complex **1**. The structure is shown in Fig. 3 and selected geometrical parameters are in Table 3. The disparity between the Si–Pt–P and Si–Pt–Si′ angles of 105.21(9) and 113.38(7)° is somewhat greater than in the nickel analogue **1**. The discrepancy between
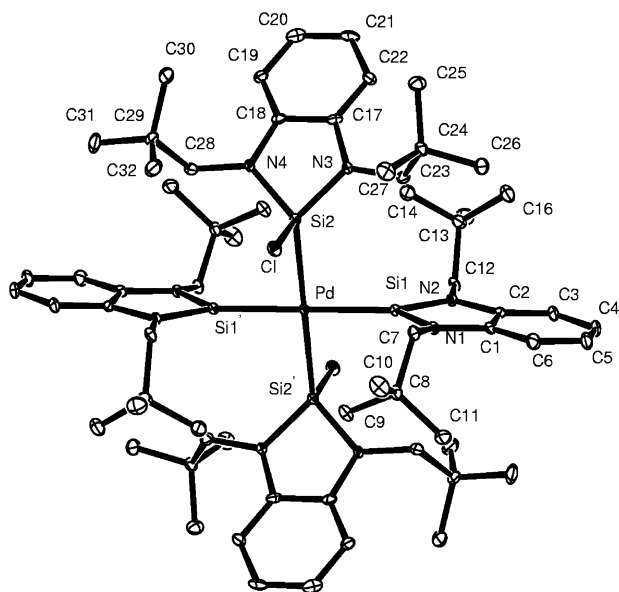

Fig. 3. Molecular structure of complex **5**.

Table 3
Selected bond lengths (Å) and angles (°) for **5**

Bond length			
Pt–Si	2.261(3)	Si–N(2)	1.737(10)
Pt–P	2.320(5)	P–C(17)	1.839(12)
Si–N(1)	1.724(10)		
Bond angles			
Si–Pt–Si′	113.38(7)	N(1)–Si–Pt	135.1(4)
Si–Pt–P	105.21(9)	N(2)–Si–Pt	131.3(4)
N(1)–Si–N(2)	89.5		

Symmetry transformations used to generate equivalent atoms: y, z, x.

the Si–Pt and P–Pt bond lengths of 2.261(3) and 2.320(5) Å, respectively, is ca. 3%; while for **1**, the corresponding bond lengths to the nickel atom vary by ca. 2%. Each silicon atom is 0.22 Å out of the

Fig. 2. Molecular structure of complex **4**.

contiguous PtN_2 plane and, as in **1**, each silylene ligand has the neopentyl substituents *cis* to one another.

Crystalline **6** has the d^{10} copper(I) atom at the centre of a distorted tetrahedron, with two of the angles at Cu near to the sp^2 value [P(2)–Cu–Si and P(2)–Cu–P(1), $118.2 \pm 1.6°$], two close to sp^3 [P(2)–Cu–I and P(1)–Cu–Si, $109.1 \pm 0.5°$] and the mean of the remaining two [Si–Cu–I and P(1)–Cu–I] is $99.6 \pm 0.6°$, Fig. 4 and Table 4. The Cu–I and the Cu–P distances are unexceptional, but slightly shorter than in [CuI(PPh$_3$)$_3$], 2.669(13) and 2.355(8) Å, respectively; in the latter each bond angle subtended at Cu is close to the sp^3 value [28]. The silicon atom in **6** is 0.26 Å out of the CuN_2 plane and, as in **1**, **2** and **3**, the two neopentyl groups are mutually cisoid.

2.5. Selected NMR spectral data for compounds **1–6**

The $^{29}Si\{^1H\}$-NMR spectral chemical shift for a solution of a transition metal silylene complex is invariably at higher frequency than in the parent silylene: SiNN, δ 96.9 [9]; SiN^{1}N^1, δ 78.3 [8]; SiN^{2}N^2, δ 119 [16]. These data are summarised in Table 5, not only for compounds **1–6** but also for the 23 others reported to date. The $^{29}Si\{^1H\}$ signal for the [SiNN(Cl)]$^-$ ligand was at much lower frequency than that for the SiNN ligand in the Pt(II) complex **3**, see below. For the Cu(I) complex **6** in C$_6$D$_6$ at ambient temperature, a $^{29}Si\{^1H\}$ signal was not detected, which we attribute to a fast (on the NMR time scale) dissociative equilibrium (in CDCl$_3$ solution the complex decomposed). For the Pd(II) complex **4** in C$_6$D$_6$ at ambient temperature, a reductive elimination process leading to Cl$_2$SiNN is indicated by the $^{29}Si\{^1H\}$-NMR spectral data, see below. The ^{195}Pt- and ^{29}Si-NMR spectra of the silyl(silylene)platinum(II) complex **3** showed that in CDCl$_3$ solution **3** underwent fluxional

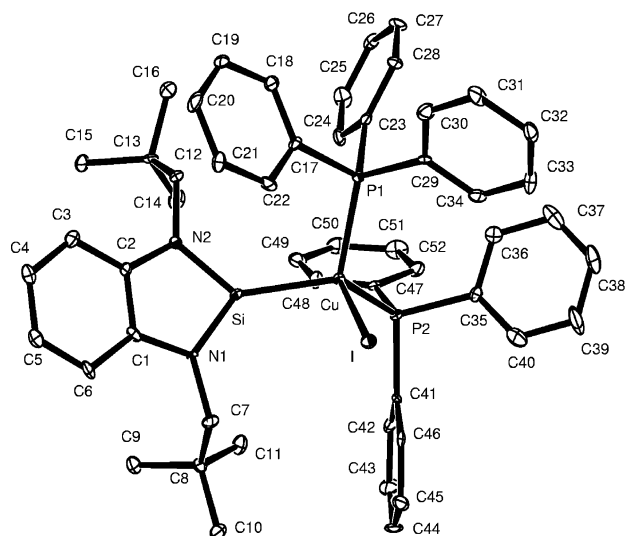Fig. 4. Molecular structure of complex **6**.

Table 4
Selected bond lengths (Å) and angles (°) for **6**

Bond lengths			
Cu–I	2.641(2)	Cu–Si	2.289(4)
Cu–P(1)	2.317(3)	Cu–P(2)	2.297(3)
Si–N(1)	1.716(9)	Si–N(2)	1.736(9)
Bond angles			
Si–Cu–P(2)	119.80(12)	Si–Cu–P(1)	108.70(13)
P(2)–Cu–I	116.60(12)	Si–Cu–I	100.22(9)
P(2)–Cu–I	109.16(9)	P(1)–Cu–I	98.98(9)
N(1)–Si–N(2)	91.1(4)	N(1)–Si–Cu	131.2(3)
N(2)–Si–Cu	131.9(3)		

processes, which have been studied by variable temperature multinuclear (^1H, $^{29}Si\{^1H\}$, $^{195}Pt\{^1H\}$), as well as ^1H saturation transfer (at 213 and 333 K) and 2D EXSY (at 243 K) NMR spectroscopy.

At 213 K, The ^1H, ^{29}Si (Fig. 6) and ^{195}Pt (Fig. 5) spectra showed the presence of three species, two major, **3a** and **3b**, and one minor, **3c**. The three ^{195}Pt chemical shifts were within the narrow range of ca. 80 ppm (δ −5474, −5497 and −5539). The ^{29}Si spectrum showed that for **3a** and **3b** there were two sets of peaks: one in the region of the coordinated silylene (δ 142.5 and 146.9, with $^1J(^{29}Si–^{195}Pt) = 2265$ and 2259 Hz, respectively) and the other in the region of the coordinated chlorosilyl ligand (δ 57.3 and 53.7, with $^1J(^{29}Si–^{195}Pt) = 957$ and 934 Hz, respectively). From the ^1H-NMR spectrum in the NCH$_2$ region it is evident that one of **3a/3b** was symmetric giving just two AB quartets, while the other showed four AB quartets. These sets of signals from the major isomers are assigned as arising from the symmetric (**3a**) and unsymmetric (**3b**), *trans*- and *cis*-square planar d^8 Pt(II) complexes, respectively.
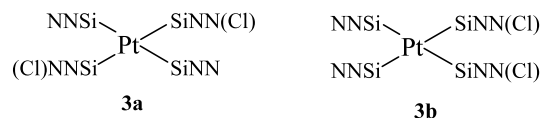
The minor isomer **3c** showed two ^{29}Si signals, both in the coordinated SiNN region (δ 143.0 and 146.5); there were none which could unambiguously be assigned to coordinated [SiNN(Cl)]$^-$. In the NCH$_2$ region of the ^1H-NMR spectrum, four AB quartets were observed which were in the low frequency region attributable to the ligand [SiNN(Cl)]$^-$; hence, we deduce that the ^{29}Si signals of this ligand were unresolved and thus undetected.

Dynamic NMR spectral experiments at 213 K (Fig. 7) showed that the lowest energy process is an exchange between the minor isomer **3c** and the *trans*-isomer **3a** *only*; this, and the close similarity of the chemical shifts for **3a** and **3c**, particularly $\delta(^{195}Pt)$, indicates that **3a** and **3c** are two versions of the *trans*-isomer which differ only in the conformation of their ligands. One possibility

Table 5
Silylene complexes of d- and f-block metals

Complex	l(M−Si) (Å)	$\delta[^{29}Si]$	Ref.	Complex	l(M−Si) (Å)	$\delta[^{29}Si]$	Ref.
[Ycp$_2$(SiNN)]	3.038(2)	119.5 at 188 K	[18]	[Ni(CO)$_2$(SiN^{1}N^1)]	2.07(2)	97.5	[15,16]
trans-[Cr(CO)$_4$(SiN^{1}N^1)$_2$]	2.329	136.9	[23]	[Ni(PPh$_3$)(SiNN)$_3$] (1)	2.165(2)	136.2	a
trans-[Cr(CO)$_4$(SiN^{2}N^2)$_2$]	2.326	170.3	[23]	[Ni(SiNN)$_4$] (2)	2.180 av.	145.9	a
trans-[Mo(CO)$_4$(SiN^{1}N^1)$_2$]	2.471	119.3	[23]	[Ni(SiN^{1}N^1)$_3$]	2.152	110.6	[22,23]
trans-[Mo(CO)$_4$(SiN^{2}N^2)$_2$]	2.480	155.3	[23]	[Ni(SiN^{2}N^2)$_3$]	2.158	144.6	[22,23]
cis-Mo(CO)$_4$(SiNN)$_2$		153.7	[34]	Pd(SiN^{1}N^1)$_3$		113.6	[24]
trans-[Mo(CO)$_4$(SiNN)$_2$]	2.4472(6)	156.5	[34]	trans-[Pd{SiNN(Cl)}$_2$(SiNN)$_2$] (4)	2.269(2) b	c	a
[MoCp$_2$(SiN^{1}N^1)]	2.4125(13)	139.3	[29]	trans-[Pt{SiNN(Cl)}$_2$(SiNN)$_2$] (3)	2.266(1) b	c	a
[MoCp*(H)(dmpe){Si(Cl)Mes}]	2.288(2)	182	[33]	[Pt(PCy$_3$)$_2$(SiMes$_2$)]	2.210(2)	358	[7]
trans-[W(CO)$_4$(SiN^{1}N^1)$_2$]	2.471	97.8	[23]	Pt(^{i}PPr)$_2$(SiMes$_2$)		367	[7]
trans-W(CO)$_4$(SiN^{2}N^2)$_2$		137.1	[23]	[Pt(PPh$_3$)(SiNN)$_3$] (5)	2.261(3)	108.4	a
trans-[Fe(CO)$_3$(SiN^{1}N^1)$_2$]	2.196	111.6	[23]	[CuI(PPh$_3$)(SiNN)] (6)	2.289(4)	c	a
trans-[Ru(CO)$_3$(SiN^{1}N^1)$_2$]	2.330	110.2	[23]	[SmCp$_2^*$(SiN^{1}N^1)]	3.1910(1)		[32]
[RuCl{CH(CH$_2$PCy$_2$)$_2$}(SiN^{1}N^1)]	2.228 av.	105.7	[30]	[YbCp$_2$(SiNN)]	2.984(2)		[18]
RuCp*(Cl)(SiN^{1}N^1)		112	[31]				

[a] This work (see also [17] for 1 and 3).
[b] This refers to M−Si(NN).
[c] See Section 2.5.
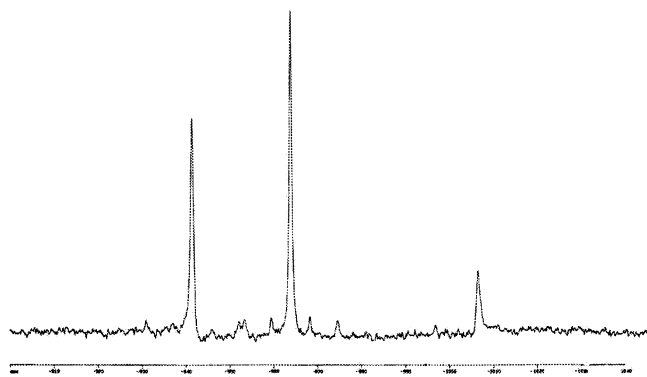
Fig. 5. ^{195}Pt{^{1}H}-NMR spectrum of 3 at 213 K.
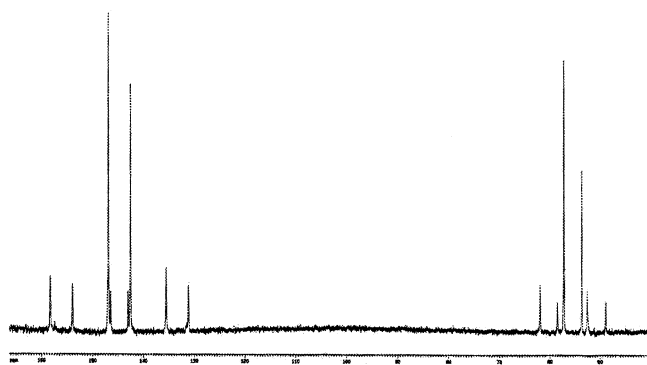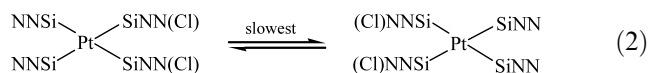

Fig. 6. ^{29}Si{^{1}H}-NMR spectrum of 3 at 213 K.

would be the rotamers of Scheme 5. (In our preliminary communication [17], we suggested that 3c was a six-coordinate Pt(II) complex; we now conclude that this is unlikely, because a six-coordinate, 20-electron Pt(II) complex would not only probably be paramagnetic but

also would be expected to have NMR spectral parameters very different from those of 3a). In summary, the structure of 3c has (i) the expected two ^{29}Si signals, while (ii) the single ^{29}SiNN(Cl) signal is assumed to be overlapping with that for 3a; and (iii) the anticipated four AB quartets, one for each of the SiNN and SiNN(Cl) ligands.

A second, but slower, dynamic process observed for complex 3 in CDCl$_3$ sets in at ca. 243 K, as illustrated by the ^{1}H-NMR 2D EXSY spectrum in the NCH$_2$ region, Fig. 8. It is attributed to the trans ⇌ cis isomerisation, Eq. (1). This may be catalysed by a trace of free silylene, implicating a five-coordinate stereochemically non-rigid platinum(II) complex Pt{SiNN(Cl)}$_2$(SiNN)$_3$} intermediate; a similar postulate is often proposed for the tertiary phosphine-catalysed cis ⇌ trans isomerisation of various d^8 [PtX$_2$(PPh$_3$)$_2$] complexes [37].

$$\qquad (1)$$
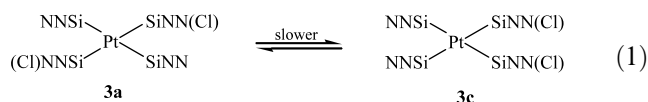
At 333 K a spin saturation ^{1}H-NMR spectral experiment showed that there was exchange between the methylene protons of the SiNN and [SiNN(Cl)]$^-$ ligands, Fig. 9. Thus, the third, and slowest of three dynamic processes, is a Si→Si 1,3-shift of Cl$^-$, illustrated in Eq. (2) for 3c.

$$\qquad (2)$$

Upon changing the solvent from CDCl$_3$ to thf-d$_8$, there was a marked shift in the cis ⇌ trans equilibrium, presumably in favour of the more polar cis-isomer.

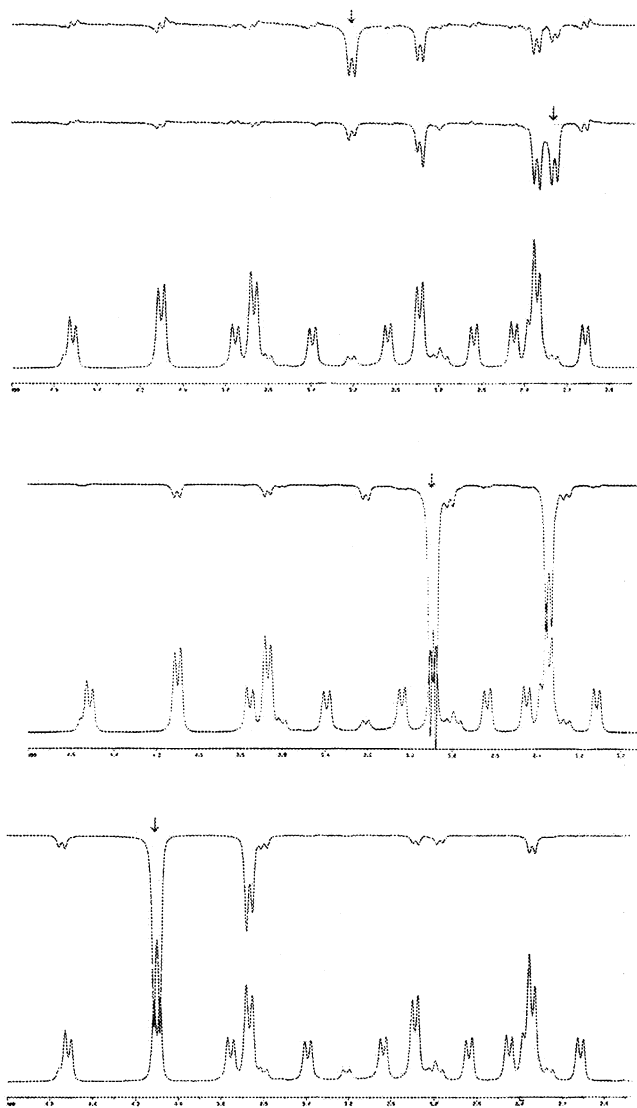Fig. 7. ^{1}H-NMR spectra of the saturation transfer study (213 K) of **3** (methylene proton region).

consistent with the notion that the reductive elimination is irreversible.

3. Conclusion

We have shown that the bis(amino)silylene $Si[(NCH_2^tBu)_2C_6H_4-1,2]$ ($\equiv$ SiNN) can behave towards a transition metal M substrate in diverse fashions: (i) it may displace CO, PR_3 or an alkene and form a complex having one or more M–SiNN bonds, (ii) such bond-formation may be accompanied by an M–X insertion reaction yielding a product having one or more M–SiNN(X) bonds, and (iii) M–SiNN bond formation may be supplemented by a reduction at the metal centre.

Type (i) reactions are illustrated here by the isolation of the d^{10} complexes **1**, **2**, **5** and **6** of Ni(0), Pt(0) and Cu(I), respectively. This type of behaviour is now widely established, as summarised in Table 5. With four exceptions, each of the listed compounds was made from a bis(amino)silylene and an appropriate transition metal substrate; those not mentioned in Sections 1 and 2 are $[MoCp_2(SiN^1N^1)]$ from $[MoCp_2(PEt_3)]$ [29], $[RuCl\{CH(CH_2PCy_2)(CH_2CH_2PCy_2)\}(SiN^1N^1)]$ from $[RuCl(L)(\mu\text{-}Cl)_3RuL(N_2)]$ $[L = Cy_2P(CH_2)_4PCy_2]$ [30], $[RuCp^*(Cl)(SiN^1N^1)]$ from $[\{RuCp^*Cl\}_4]$ [31], and $[SmCp_2^*(SiN^1N^1)]$ [32]. The exceptions are $[MoCp^*(H)-(dmpe)\{Si(Cl)Mes\}]$, obtained from $[MoCp^*(\eta^3\text{-}CH_2Ph)(dmpe)]$ and $SiH_2(Cl)Mes$ [33]; the crystalline *trans*-$[Mo(CO)_4(SiNN)_2]$ (in equilibrium in solution with the *cis*-isomer), formed by heating **7**, with $[Mo(CO)_3\{\eta\text{-}[C(^tBu)P]_3\}]$ as coproduct [34]; and the $[Pt(PR_3)_2(SiMes_2)]$ [7] complexes mentioned in Section 1.
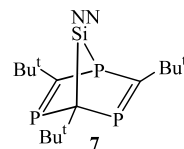
The type (ii) reactions are exemplified here by the isolation of the crystalline d^8 Pt(II) (**3**) and Pd(II) (**4**) complexes, with the former more robust than the latter; complex **3** has been shown to undergo three distinct fluxional processes in solution. It appears that only two other examples of insertion reactions have been reported, Eq. (3) (M = Mo, W), but they differ from (ii) in that they relate to the conversion of a silylene into a silylmetal product [29].

$$[MCp_2H_2 + SiN^1N^1 \xrightarrow{M=Mo \text{ or } W} [MH(Cp)_2\{SiN^1N^1(H)\}] \quad (3)$$
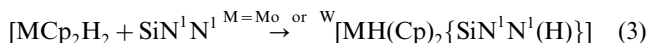
Nevertheless, we predict that many more M–X/SiX$_2$ insertion reactions remain to be discovered, e.g., involving a d^8-$(\mu\text{-}Cl)_2M_2$ precursor [M = Rh(I) or Pt(II)].
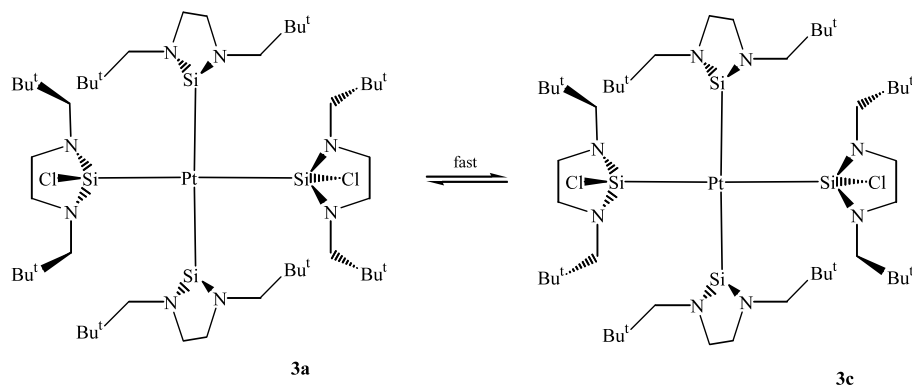
The palladium(II) complex **4** in C_6D_6 solution is evidently (and not unexpectedly [24]) more labile than its isoleptic Pt(II) analogue **3**. Thus, the $^{29}Si\{^1H\}$-NMR spectrum of **4** in C_6D_6 at 298 K showed three signals in the NNSi-metal region (at δ 132.1, 133.6 and 134.7, in an intensity ratio of ca. 1:2:1) and one at δ 24.1, which corresponds to the literature value for Cl_2SiNN [20]. The formation of the latter is indicative of a reductive elimination of **4**, yielding a mixture of (or a single) silylene-Pd(0) complexes of as yet unknown composition. One possible interpretation of the three signals is that two are from *trans*- and *cis*-$[Pd\{SiNN-(Cl)\}_2(SiNN)_2]$ (although a signal characteristic of $\{SiNN(Cl)\}^-$ was not observed) and the third due to $Pd(SiNN)_n$. Several attempts to recrystallise **4** failed,

Scheme 5.

Fig. 8. ^{1}H-NMR 2D EXSY spectrum of 3 (243 K, methylene proton region).

Fig. 9. ^{1}H-NMR spectra of the saturation transfer study (333 K).

Type (iii) reactions are revealed here in the formation of the d^{10} Ni(0) complexes 1 and 2 from the d^8 precursor [NiCl$_2$(PPh$_3$)$_2$] or NiCl$_2$, the SiNN acting not only as a ligand but also a dechlorinating reagent, Cl$_2$SiNN being the coproduct. Other examples are not yet in the literature, but readily reducible d-metal chlorides or heavier halides are likely targets, e.g., an appropriate Ti(IV) chloride or a Pd(II) bromide.

The bis(amino)silylenemetal complexes have ^{29}Si chemical shifts (Table 5) at higher frequency than in the parent SiNN (δ 96.9), SiN^{1}N^1 (δ 78.3) and SiN^{2}N^2 (δ 119), but at significantly lower frequency than in [Pt(PR$_3$)$_2$(SiMes$_2$)] (R = ^{i}Pr, Cy); although the other α-amino-free silylenemetal complex [MoCp*(H)(dmpe){Si(Cl)Mes}] has the relatively low frequency δ[^{29}Si] value of 182 ppm [33]. As for relative values of δ[^{29}Si] in related M–SiNN, M–SiN^{1}N^1 and M–SiN^{2}N^2

complexes, data for only one series are available, namely trans-[Mo(CO)$_4$(SiX$_2$)$_2$] in which δ[^{29}Si] decrease in the sequence SiNN $\geq$ SiN^{2}N^2 $\gg$ SiN^{1}N^1; the relative position of SiN^{1}N^1 and SiN^{2}N^2 complexes is also maintained for appropriate Cr(0), W(0) and Ni(0) series [23].

The crystalline homoleptic d^{10} bis(amino)silylene-nickel(0) complexes have a four-(SiNN) (2) or three-(SiN^{1}N^1 or SiN^{2}N^2) coordinate metal environment, whence it appears [23] that the non-benzenoid ligands with the N^{t}Bu substituent are sterically the more crowded.

The M–SiX$_2$ bond for bis(amino)silylene ligands probably has a predominant σ-component, with only a rather weak $_{\pi\text{-}M}\overset{\bullet\bullet}{\frown}_{Si}$ contribution. This is consistent with (i) comparative IR and NMR spectral data for carbonylmetal silylene complexes [23], (ii) molecular orbital calculations on model compounds Cl–M–SiN^{3}N^3 (M = Cu, Ag, Au; SiN^{3}N^3 = Si[N(H)CH]$_2$) [35], (iii) comparisons with related triarylphosphine-, E[N(SiMe$_3$)$_2$]$_2$– (E = Ge or Sn) and C[N(Me)CH$_2$]$_2$– [36] metal complexes, and (iv) the observation that in each of 1–6 the silicon atom of the silylene ligand is out of the MN$_2$ plane.

Finally, we note that the neopentyl substituents at the nitrogen of M–SiNN moieties are disposed *cis* in **1**, **2**, **5** and **6**, but *trans* in **3** and **4**.

4. Experimental

4.1. Materials and procedures

All operations and manipulations were carried out under purified argon, by conventional Schlenk techniques. Solvents were dried and degassed before use. The NMR spectra were recorded in C_6D_6 or $CDCl_3$ using Bruker Instruments: Bruker DPX 300 (^{1}H at 300 MHz, ^{13}C at 75.5 MHz and ^{31}P at 121.5 MHz) and AMX 500 (^{1}H at 500 MHz and [29]Si at 49.7 MHz), and referenced internally to residual solvent resonances in the case of [1]H- and ^{13}C-spectra, or externally to H_3PO_4 or $SiMe_4$ for ^{31}P and [29]Si, respectively; data in δ. Microanalyses were carried out by Medac Ltd. (Brunel University). Melting points were taken in sealed capillaries and are uncorrected. The yield of the products were not optimised. The inorganic starting materials, with one exception, were purchased from STREM, while $Si[(NCH_2^tBu)_2C_6H_4-1,2]$ [9] and $[CuI(PPh_3)_3]$ [28] were prepared as described in the literature.

4.2. Reaction of **SiNN** with [NiCl2(PPh3)2] (ratio 4:1)

A solution of **SiNN** (0.38 g, 1.4 mmol) in benzene (20 ml) was added to a solution of $[NiCl_2(PPh_3)_2]$ (0.23 g, 0.35 mmol) in benzene (20 ml) and stirred for several hours. After removal of the solvent in vacuo the residue was dissolved in pentane and cooled to $-25\,^{\circ}C$ to afford yellow crystals of **1** (0.27 g, 68%), m.p. 105–108 $^{\circ}C$ (dec.). ^{1}H-NMR (C_6D_6): δ 0.78 (s, 54H, CH_3), 3.26 (s, 12H, CH_2), 6.96 (m, 21H, phenyl) and 7.70 (m, 6H, phenyl). ^{13}C{^{1}H}-NMR (C_6D_6): δ 29.46 (CMe_3), 34.08 (CMe_3), 52.47 (CH_2), 110.99, 117.52 and 141.22 (phenyl). ^{31}P{^{1}H}-NMR (C_6D_6): δ 47.31 (s). ^{29}Si{^{1}H}-NMR (C_6D_6): δ 136.19. Anal. Calc. for $C_{66}H_{93}N_6NiPSi_3$: C, 69.3; H, 8.19; N, 7.34; Found: C, 68.9; H, 8.43; N, 7.41%.

4.3. Reaction of **SiNN** with [NiCl2(PPh3)2] (ratio 5:1)

Using the procedure in Section 4.2, but with **SiNN** (0.40 g, 1.5 mmol) and $[NiCl_2(PPh_3)_2]$ (0.19 g, 0.3 mmol) and crystallisation from hexane afforded at $-25\,^{\circ}C$ yellow crystals of **2** (suitable crystals for X-ray from Et_2O) (0.23 g, 66%), m.p. 84–86 $^{\circ}C$ (dec.). ^{1}H-NMR (C_6D_6): δ 0.87 (s, 72H, CH_3), 3.76 (s, 16H, CH_2), 6.96 (m, 8H, phenyl) and 7.08 (m, 8H, phenyl). ^{13}C{^{1}H}-NMR (C_6D_6): δ 29.94 (CMe_3), 34.32 (CMe_3), 52.96 (CH_2), 110.84, 118.06 and 141.30 (phenyl). ^{29}Si{^{1}H}-NMR (C_6D_6): δ 145.9. Anal. Calc. for $C_{64}H_{104}N_8NiSi_4$:

C, 66.5; H, 9.06; N, 8.68. Found: C, 64.4; H, 8.57; N, 8.27%.

4.4. Reaction of **SiNN** with [Ni(cod)2]

A solution of **SiNN** (0.85 g, 3.1 mmol) in benzene (20 ml) was added to a solution of $[Ni(cod)_2]$ (0.21 g, 0.76 mmol) in benzene (20 ml) and stirred for several hours. After removal of the solvent in vacuo the residue was recrystallised from hexane yielding yellow crystals of **2** (0.81 g, 92%).

4.5. Reaction of **SiNN** with NiCl2

A solution of **SiNN** (0.84 g, 3.08 mmol) in benzene (20 ml) was added to a suspension of an excess of $NiCl_2$ (0.2 g, 1.54 mmol). After stirring for several hours the mixture was filtered and the solvent was removed in vacuo. Crystallisation from hexane at $-25\,^{\circ}C$ gave yellow crystals of **2** (0.47 g, 66%).

4.6. Reaction of **SiNN** with [PdCl2(PPh3)2]

A solution of **SiNN** (0.59 g, 2.15 mmol) in benzene (20 ml) was added to a solution of $[PdCl_2(PPh_3)_2]$ (0.3 g, 0.43 mmol) in benzene (20 ml). After stirring the mixture for several hours a small amount of crystalline solid formed. The solution was stored at 15 $^{\circ}C$ to complete crystallisation; this yielded bright orange crystals of **4** (0.44 g, 80%), m.p. 115–117 $^{\circ}C$ (dec.). For NMR data see text. Anal. Calc. for $C_{64}H_{104}Cl_2N_8PdSi_4\cdot5C_6H_6$: C, 67.8; H, 8.11; N, 6.73. Found: C, 67.1; H, 7.92; N, 7.4%.

4.7. Reaction of **SiNN** with [PdCl2(cod)]

A solution of **SiNN** (0.70 g, 2.55 mmol) in benzene (20 ml) was added to a solution of $[PdCl_2(cod)]$ (0.15 g, 0.51 mmol) in benzene (20 ml) and stirred for several hours. Orange crystals of **4** (0.59 g, 91%), were obtained.

4.8. Reaction of **SiNN** with [PtCl2(PPh3)2]

A solution of **SiNN** (0.3 g, 1.0 mmol) in benzene (20 ml) was added to a solution of $[PtCl_2(PPh_3)_2]$ (0.16 g, 0.2 mmol) in benzene (20 ml). After removal of the solvent in vacuo the residue was crystallised at $-25\,^{\circ}C$ from hexane to afford orange crystals of **3** (0.16 g, 58%), m.p. 158–161 $^{\circ}C$ (dec.). X-ray-suitable crystals were obtained from benzene. For NMR data see text. Anal. Calc. for $C_{64}H_{104}Cl_2N_8PtSi_4$: C, 56.4; H, 7.69; N, 8.21. Found: C, 58.5; H, 7.42; N, 7.22%.

4.9. Reaction of **SiNN** with [PtCl2(cod)]

A solution of **SiNN** (0.52 g, 1.9 mmol) in benzene (20 ml) was added to a solution of $[PtCl_2(cod)]$ (0.14 g, 0.38

mmol) in benzene (20 ml) and stirred for several hours. After removal of the solvent in vacuo the residue was crystallised from hexane yielding orange crystals of **3** (0.46 g, 89%).

4.10. Reaction of **SiNN** with [Pt(PPh₃)₄]

A solution of **SiNN** (0.21 g, 0.75 mmol) in benzene (10 ml) was added to a solution of [Pt(PPh₃)₄] (0.18 g, 0.15 mmol) in benzene (10 ml) and stirred for 16 h. The solvent was removed in vacuo. The residue was extracted with hexane, which led to the precipitation of PPh₃. After filtration and removal of the solvent in vacuo the residue was crystallized from diethyl ether at $-25\,^{\circ}$C yielding a few orange crystals of **5** (0.09 g). ^{1}H-NMR (C₆D₆): δ 0.84 (s, 54H, CH₃), 3.25 (vbr s, 12H, CH₂), 6.93 (m, 21H, phenyl) and 7.63 (m, 6H, phenyl). ^{31}P{^{1}H}-NMR (C₆H₆): δ 22.85 ($^{1}J_{P,Si}$ 1587 Hz). ^{29}Si{^{1}H}-NMR (C₆D₆): δ 108.4.

4.11. Reaction of **SiNN** with [CuI(PPh₃)₃]

A solution of **SiNN** (0.37 g, 1.35 mmol) in benzene (20 ml) was added to a solution of [CuI(PPh₃)₃] (0.88 g, 0.9 mmol) in benzene (20 ml) and stirred for 16 h. After removal of the solvent in vacuo the residue was extracted into diethyl ether. The extract was filtered and after ca. 1/2 h some white precipitate had formed; the mixture was filtered again. The filtrate was stored at ambient temperature for several days to afford yellow crystals of **6** (0.65 g, 73%), m.p. 189–190 $^{\circ}$C. ^{1}H-NMR (C₆D₆): δ 0.91 (s, 18H, CH₃), 3.78 (s, 4H, CH₂), 6.98 (m, 22H, phenyl) and 7.58 (m, 12H, phenyl). ^{13}C{^{1}H}-NMR (C₆D₆): δ 28.73 (C*Me*₃), 33.47 (*C*Me₃), 53.91 (CH₂), 111.25, 118.85 and 140.48 (phenyl), 128.63 (d), 129.47,

134.53 (d) and 135.33 (d) (PPh₃). Anal. Calc. for C₅₂H₅₆CuIN₂P₂Si: C, 63.1; H, 5.70; N, 2.83. Found: C, 62.9; H, 6.01; N, 2.77%.

4.12. X-ray structure determinations for the complexes **2**, **4**, **5** and **6**

Data for the crystal structure determinations were collected on an Enraf-Nonius CAD4 diffractometer at 173(2) K using monochromated Mo–K$_{\alpha}$ radiation (λ 0.71073 Å). The structures were solved by direct methods using SHELXL-86 [38] and refined by full-matrix least squares on F^2 using SHELXL-93 [39] for **2**, **4** and **5**, or SHELXL-97 [40] for both structure solution and refinement for **6**, with all non-H atoms anisotropic; H's were included in riding mode with U_{iso}(H) = 1.2 U_{eg}(C) or 1.5 U_{eq}(C) for methyl groups. Crystal data and refinement details are listed in Table 6.

5. Supplementary material

Crystallographic data for the structural analysis have been deposited with the Cambridge Crystallographic Data centre, CCDC no. 207542 for compound **2**, CCDC no. 207543 for compound **4**, CCDC no. 207544 for compound **5**, and CCDC no. 207545 for compound **6**. Copies of this information may be obtained free of charge from The Director, CCDC, 12 Union Road, Cambridge CB2 1EZ, UK (Fax: +44-1223-336033; e-mail: deposit@ccdc.cam.ac.uk or www: http://www.ccdc.cam.ac.uk).

Table 6
Crystal data and refinement for complexes **2**, **4**, **5** and **6**

	2	4	5	6
Formula	C₆₄H₁₀₄N₈NiSi₄·(C₄H₁₀O)	C₆₄H₁₀₄Cl₂N₈PdSi₄·5(C₆H₆)	C₆₆H₉₃N₆PPtSi₃	C₅₂H₄₆CuIN₂PSi·0.5(C₄H₁₀O)
M	1230.7	1665.75	1280.8	1016.4
Crystal system	Orthorhombic	Triclinic	Cubic	Triclinic
Space group	$Pbca$ (No. 61)	$P\bar{1}$ (No. 2)	$Pa3$ (No. 205)	$P\bar{1}$ (No. 2)
a (Å)	20.780(4)	13.757(7)	24.026(4)	13.409(6)
b (Å)	26.188(7)	13.874(5)	24.026(4)	14.083(6)
c (Å)	26.922(6)	13.982(5)	24.026(4)	15.308(14)
α (°)	90	85.35(3)	90	87.340(5)
β (°)	90	61.02(3)	90	78.680(6)
γ (°)	90	77.34(3)	90	62.710(14)
U (Å³)	14 651(6)	2277(2)	13 869(4)	2516(3)
Z	8	1	8	2
Unique reflections collected	12 823	6313	2828	6142
Reflections with $I > 2\sigma(I)$	7448	4048	1787	3953
Data/restraints/parameters	12 822/0/739	6313/0/490	2828/0/232	6142/0/568
Goodness-of-fit on F^2	1.015	1.054	1.421	1.008
Final R indices [$I > 2\sigma(I)$]	$R_1 = 0.070$, $wR_2 = 0.152$	$R_1 = 0.059$, $wR_2 = 0.097$	$R_1 = 0.056$, $wR_2 = 0.141$	$R_1 = 0.071$, $wR_2 = 0.158$
R indices (all data)	$R_1 = 0.138$, $wR_2 = 0.190$	$R_1 = 0.117$, $wR_2 = 0.120$	$R_1 = 0.101$, $wR_2 = 0.156$	$R_1 = 0.126$, $wR_2 = 0.187$

Acknowledgements

References

[1] T.D. Tilley, in: S. Patai, Z. Rappoprt (Eds.), The Chemistry of Organic Silicon Compounds, Wiley, New York, 1989, p. 1415.

[2] C. Zybill, Top. Curr. Chem. 160 (1992) 1.

[3] P.D. Lickiss, Chem. Soc. Rev. (1992) 271.

[4] D.A. Straus, S.D. Grumbine, T.D. Tilley, J. Am. Chem. Soc. 112 (1990) 7801.

[5] S.R. Klei, T.D. Tilley, R.G. Bergman, J. Am. Chem. Soc. 122 (2000) 1816.

[6] S.D. Grumbine, T.D. Tilley, F.P. Arnold, A.L. Rheingold, J. Am. Chem. Soc. 115 (1993) 7884.

[7] J.D. Feldman, G.P. Mitchell, J.O. Nolte, T.D. Tilley, J. Am. Chem. Soc. 120 (1998) 11184.

[8] M. Denk, R. Lennon, R. Hayashi, R. West, A.V. Belyakov, H.P. Verne, A. Haaland, M. Wagner, N. Metzler, J. Am. Chem. Soc. 116 (1994) 2691.

[9] B. Gehrhus, M.F. Lappert, J. Heinicke, R. Boese, D. Bläser, J. Chem. Soc. Chem. Commun. (1995) 1931.

[10] M. Haaf, T.A. Schmedake, R. West, Acc. Chem. Res. 33 (2000) 704.

[11] B. Gehrhus, M.F. Lappert, J. Organomet. Chem. 617 (2001) 209.

[12] W.A. Herrmann, C. Kocher, Angew. Chem. Int. Ed. Engl. 36 (1997) 2163.

[13] A.J. Arduengo, R. Krafczyk, Chem. Unserer Zeit 32 (1998) 6.

[14] M.F. Lappert, R.S. Rowe, Coord. Chem. Rev. 100 (1990) 267.

[15] M. Denk, R.K. Hayashi, R. West, J. Chem. Soc. Chem. Commun. (1994) 33.

[16] R. West, M. Denk, Pure Appl. Chem. 68 (1996) 785.

[17] B. Gehrhus, P.B. Hitchcock, M.F. Lappert, H. Maciejewski, Organometallics 17 (1998) 5599.

[18] X.P. Cai, B. Gehrhus, P.B. Hitchcock, M.F. Lappert, Can. J. Chem. Rev. Can. Chim. 78 (2000) 1484.

[19] T.A.K. Al-Alaf, C. Eaborn, P.B. Hitchcock, M.F. Lappert, A. Pidcock, J. Chem. Soc. Chem. Commun. (1985) 548.

[20] B. Gehrhus, P.B. Hitchcock, M.F. Lappert, J. Heinicke, R. Boese, D. Bläser, J. Organomet. Chem. 521 (1996) 211.

[21] P.B. Hitchcock, M.F. Lappert, M.C. Misra, J. Chem. Soc. Chem. Commun. (1985) 863.

[22] T.A. Schmedake, M. Haaf, B.J. Paradise, D. Powell, R. West, Organometallics 19 (2000) 3263.

[23] T.A. Schmedake, M. Haaf, B.J. Paradise, A.J. Millevolte, D.R. Powell, R. West, J. Organomet. Chem. 636 (2001) 17.

[24] W.A. Herrmann, P. Härter, W.K. Gstöttmayer, F. Bielert, N. Seeboth, P. Sirsch, J. Organomet. Chem. 649 (2001) 141.

[25] A. Fürstner, H. Krause, C.W. Lehmann, Chem. Commun. (2001) 2372.

[26] Y. Tanaka, H. Yamashita, S. Shimada, M. Tanaka, Organometallics 16 (1997) 3246.

[27] M. Murakami, T. Yoshida, S. Kawanami, Y. Ito, J. Am. Chem. Soc. 117 (1995) 6408.

[28] P.F. Barron, J.C. Dyason, P.C. Healy, L.M. Engelhardt, C. Pakawatchai, V.A. Patrick, A.H. White, J. Chem. Soc. Dalton. Trans. (1987) 1099.

[29] S.H.A. Petri, D. Eikenberg, B. Neumann, H.-G. Stammler, P. Jutzi, Organometallics 18 (1999) 2615.

[30] D. Amoroso, M. Haaf, G.P.A. Yap, R. West, D.E. Fogg, Organometallics 21 (2002) 534.

[31] J.M. Dysard, T.D. Tilley, Organometallics 19 (2000) 4726.

[32] W.J. Evans, J.M. Perotti, J.W. Ziller, D.F. Moser, R. West, Organometallics 22 (2003) 1160.

[33] B.V. Mork, T.D. Tilley, Angew. Chem. Int. Edit. 42 (2003) 357.

[34] S.B. Clendenning, B. Gehrhus, P.B. Hitchcock, D.F. Moser, J.F. Nixon, R. West, J. Chem. Soc. Dalton. Trans. (2002) 484.

[35] C. Boehme, G. Frenking, Organometallics 17 (1998) 5801.

[36] M.F. Lappert, J. Organomet. Chem. 358 (1988) 185.

[37] F.R. Hartley, The Chemistry of Platinum and Palladium, Applied Science Publishers Ltd, London, 1973, pp. 313–315.

[38] G.M. Sheldrick, SHELXS-86, Program for the Solution of Crystal Structures, University of Göttingen, Germany, 1985.

[39] G.M. Sheldrick, SHELXL 93, Program for Crystal Structure Refinement, University of Göttingen, Germany, 1993.

[40] G.M. Sheldrick, SHELXL 97, Program for Crystal Structure Refinement, University of Göttingen, Germany, 1997.